AN INVESTIGATION ON THE PERFORMANCE OF AN IMIDAZOLINE BASED COMMERCIAL CORROSION INHIBITOR ON CO_2 CORROSION OF MILD STEEL

A. Khavasfar

Department of Materials Science and Metallurgical Engineering
Shahid Bahonar University of Kerman, Kerman, Iran
ali_khavasfar@yahoo.com

M. H. Moayed*

Department of Materials and Metallurgical Engineering, Faculty of Engineering
Ferdowsi University of Mashhad, P.O. Box 91775-1111, Mashhad, Iran
mhmoayed@um.ac.ir

A. H. Jafari

Department of Materials Science and Metallurgical Engineering
Shahid Bahonar University of Kerman, Kerman, Iran
jafari_hamid2002@yahoo.com

*Corresponding Author

(**Received: December 11, 2005 - Accepted in Revised Form: January 18, 2007)**

Abstract The performance of an Imidazoline based commercial corrosion inhibitor on CO_2 corrosion of mild steel was investigated in a Cl^- containing solution employing linear polarization resistance (LPR), potentiodynamic polarization and monitoring corrosion potential techniques. Experimental results showed that an increase of the commercial inhibitor concentration up to 500ppm increases the R_P value and produces an efficiency of 90 percent. The increase of a test solution temperature at 60°C caused an increase on R_P value compared to R_P measured at room temperature this suggests adsorption of the inhibitor is promoted by temperature. Plot of c/θ versus inhibitor concentration (c) using different methods showed a straight line with a slope very close to unity, indicating that adsorption of the investigated commercial inhibitor on steel/saturated CO_2 solution obeys the Lungmuir adsorption isotherm.

Keywords CO_2 Corrosion, Corrosion Inhibitor, Linear Polarization Resistance, Potentiodynamic Polarization, Lungmuir Adsorption Isotherm

چکیده عملکرد یک بازدارنده تجاری خوردگی با بکارگیری تکنیک های پلاریزاسیون خطی، پلاریزاسیون با پتانسیل متغیر و اندازه گیری تغییرات پتانسیل خوردگی با زمان در مورد خوردگی CO_2 فولاد ساده کربنی در محلول حاوی یون کلر مورد مطالعه قرار گرفته است. نتایج بدست آمده بیانگر بازدهی ۹۰ درصد در غلظت ۵۰۰ پی پی ام و افزایش شیب پلاریزاسیون خطی (R_P) با افزایش غلظت بازدارنده می باشد. مقایسه شیب پلاریزاسیون خطی بدست آمده در دمای محیط با این شیب در دمای ۶۰°C بیانگر بهبود جذب سطحی بازدارنده با افزایش دما می‌باشد. رفتار خطی با شیب نزدیک به واحد تغییرات (c/θ) بر حسب غلظت بازدارنده (c) از اطلاعات بدست آمده از روشهای مختلف نشان داد که جذب سطحی بازدارنده تجاری مورد استفاده از جذب ایزوترم لانگموئر تبعیت می‌کند.

1. INTRODUCTION

Carbon dioxide (CO_2) corrosion is a great problem in the extraction, production and transport of oil and natural gas [1]. Carbon and low alloy steels are the most commonly used construction materials for

oil and gas industries. They are, however, very susceptible to corrosion in environments containing CO_2. There are many variables associated with the CO_2 corrosion process such as PH, temperature, pressure, flow regime, steel composition, inhibitor, brine chemical composition, the nature of surface films and etc [2]. When CO_2 dissolves in the water, carbonic acid forms which is corrosive to carbon steel:

$$CO_2 + H_2O \Leftrightarrow H_2CO_{3(aq)} \quad (1)$$

Several mechanisms have been proposed for the dissolution of iron in aqueous, deareted CO_2 solutions [1-8]. The main corrosion process is controlled by the three following electrochemical cathodic reactions that are supported by an anodic reaction. Since CO_2 corrosion occurs in anaerobic (oxygen free) conditions, oxidation of ferrous to ferric ions is not proposed [3-5].

$$2H_2CO_3 + 2e^- \longrightarrow H_2 + 2HCO_3^- \quad E^\circ = -0.662\ V_{SCE} \quad (2a)$$

$$2H_2CO_3^- + 2e^- \longrightarrow 2H_2 + 2CO_3^{-2} \quad E^\circ = -0.856\ V_{SCE} \quad (2b)$$

$$2H^+ + 2e^- \longrightarrow H_2 \quad E^\circ = -0.481\ V_{SCE} \quad (2c)$$

$$Fe \longrightarrow Fe^{+2} + 2e \quad E^\circ = -0.680\ V_{SCE} \quad (3)$$

Considering pH value of 3.8 for saturated concentration CO_2 environments, reduction reaction of protons to hydrogen atoms equilibrates at a potential of-0.481 V (SCE). On the other hand standard equilibrium reversible potential of (2a) and (2b) cathodic reactions that are very much lower than the reduction reaction of protons suggests that reduction of H_2CO_3 and HCO_3^- to hydrogen are thermodynamically more difficult than the classical $2H^+ + 2e^- \rightarrow H_2$ cathodic reaction [5]. Due to these processes, a corrosion layer is formed on the steel surface. The property of this layer is an important factor that should be taken into account in the CO_2 corrosion. The following reactions have been suggested for $FeCO_3$ formation.

$$Fe^{+2} + CO_3^{-2} \longrightarrow FeCO_3 \quad (4)$$

$$Fe^{+2} + 2HCO_3^- \longrightarrow Fe(HCO_3)_2 \quad (5a)$$

$$Fe(HCO_3)_2 \longrightarrow FeCO_3 + CO_2 + H_2O \quad (5b)$$

The acceleration effect of CO_2 can be explained by the fact that CO_2 increases the rate of electrochemical reduction reactions generated by H^+ and H_2CO_3 species [6]. Although in CO_2 solutions with higher pH values, the direct reduction of bicarbonate ion becomes the predominant cathodic reaction [7].

X-ray photoelectron spectroscopy (XPS), scanning electron microscopy (SEM) and X-ray diffraction (XRD) were employed by S.L Wu et al. [1] to systematically characterize the chemical composition and the microstructure surface film on N80 oil tube steel exposed to CO_2 corrosion. It was reported that the main phase in the surface film was a complex carbonate mainly of iron carbonate - $(Fe,Ca)CO_3$ - as a result of isomorphism combination between $CaCO_3$ (calcite) and $FeCO_3$ (siderite). Another study was carried out by S.L. Wu and co-workers on the protective ability of the surface film on carbon steel in CO_2 environment employing electrochemical impedance spectroscopy (EIS) [4]. It was found that the protective performance of the surface film was enhanced with an increase of the exposure time period of 0-96 hr. The surface film that formed at a high temperature (150°C) was more protective than that which formed at a low temperature (60°C) due to the change in the nature of the surface film. The film formed at a higher temperature was more compact and continuous. In another investigation, Dugstrad examined the film morphology evolution on mild steel exposed to CO_2 corrosion in different temperatures [8]. Below 40°C, the surface films present an open porous structure and are formed mainly of Fe_3C with some $FeCO_3$ and alloying elements of steel. The Fe_3C is as former part of the original steel in the non-oxidized state that accumulates on the surface as the corrosion of the steel proceeds. Here the corrosion rate

decrease with time for the first three days, but it decreases again for the next six days, an effect attributed to Fe_3C, which is suggested to increase the cathodic reaction. At 60°C, the films present an inner porous layer mainly Fe_3C with more $FeCO_3$ accumulate at the outer part. However the formation of $FeCO_3$ did not reduce the corrosion rate significantly. At 80°C, a dense protective $FeCO_3$ is formed close to the metal and it decreases the corrosion rate quickly. Corlet and co workers [9,10] suggested that $FeCO_3$ can precipitate not only on steel, but directly on Fe_3C , this is due to Fe^{+2} concentration and the additional HCO_3^- ions produced on Fe_3C by cathodic reduction reaction of CO_2.

Organic corrosion inhibitors are the most effective means of protection to sever internal corrosion of carbon steel construction in the oil and gas industry. Nitrogen-based organic surfactants such as imidazoline amids (IM), imidazoline amido amines (IO) and their derivative salts have been successfully used as inhibitors in oil and gas applications even without an understanding of the facts on the inhibition mechanism and performance of these inhibitors [11]. In order to investigate the inhibitive performance and mechanism of these inhibitors, various electrochemical techniques [12-14] in different solution hydrodynamic conditions [14,15] have been investigated in detail. The performance of benzimidazole as a corrosion inhibitor in CO_2 environments was studied by D.A. Lopez and co-workers [16] employing Electrochemical Impedance Spectroscopy (EIS) and Linear Polarization Resistance (LPR) techniques. Carbon steel with two different microstructures (annealed and quenched-tempered \Q and T) was used in a deoxygenated 5 % wt. NaCl solution which was saturated with CO_2 at 40°C. Their results showed that without an inhibitor, the Q and T specimen showed a better corrosion resistance than the annealed one. The presence of a corrosion inhibitor improved the corrosion resistance of the annealed sample whereas for Q and T samples the opposite behavior was observed. It was proposed that the protection mechanism of benzimidazole is based on the reduction of protonated species at the cathodic sites (Fe_3C), leading to adsorption and blockage of these active areas and a relatively small delay in $FeCO_3$ precipitation. They concluded that the corrosion process and inhibitor efficiency is affected by heat treatment applied on the steel. The inhibition mechanism and adsorption/desorption of imidazoline amid (IM) on iron surfaces in saline solution saturated with 0.1 MPa CO_2 was investigated by X. Zhang and co-workers [17] employing EIS and potentiodynamic polarization techniques. They defined an adsorption potential in the potentiodynamic polarization curve of iron in a test environment. When the potential is greater than adsorption potential, IM will be adsorbed from the electrode surface and results in an increase in interface capacitance (C_{dl}) and a decrease in transmission resistance ($R_{c.t}$). The increase of temperature and addition of chloride ions into the solution decreases the adsorption potential of IM on iron surface. The inhibition mechanism of an imidazoline based inhibitor under multiphase flow conditions using a large diameter flow loop system was studied by Y. Chen and co-workers [14]. They employed the EIS technique and from quantitative analyzing through the Warburg parameter (b_f) they were able to determine conditions for inhibitor film formation on steel surfaces. They expressed that the inhibitor film formation is correlated to exposure time and inhibitor concentration. The film becomes less porous with the increase in exposure time and inhibitor concentration. The turbulent flow at the high rate of turbulence and bubble impact can degrade the inhibitor performance and increase the corrosion rate.

In this study, the inhibition performance of an Imidazoline based commercial grade inhibitor that is widely used in petrochemical industries is examined using electrochemical techniques. The effect of environment temperatures, inhibitor concentration and exposure time on the inhibitor performance is the aim of this work.

2. EXPERIMENTAL PROCEDURE

2.1. Specimen Preparation The working electrode was selected from a gas well tubing steel (composition given in Table 1) with a surface area of 1.35 cm^2 for all measurements. Each specimen was soldered to copper wire for electrical connection. The copper wire was covered with a

PVC tube to provide insulation from the test environment. Specimens were mounted in resin, and allowed to set overnight in air. All specimens were mechanically wet polished with a 600 grit SiC paper, then degreased with acetone prior to drying with air. Those specimens that were used in the morphological investigation by scanning electron microscopy (SEM) were mechanically polished up to 3μm and then etched by Nital.

2.2. Test Solution The salt water solution contains 96.2 gr/lit NaCl, 3.3 gr/lit $CaCl_2$ and 1.8 gr/lit $MgCl_2$ a mixture that is proposed by NACE 1D-182 simulating gas well solution [18]. The test solution was deoxygenated with Ar gas for 3 hours to remove the dissolved O_2 in the solution and then was saturated with CO_2 gas for 3 hours. To make sure that the solution was saturated with CO_2, the pH of the solution was measured prior to each test run. A pH value of 3.8 is acceptable [17,19]. The test solution was kept under a CO_2 atmosphere during testing. A commercial Imidazoline based inhibitor was used in this work. The effect of temperature on the inhibition efficiency of the inhibitor was investigated at 60°C using bathwater. All experiments were conducted in 1000 ml beaker. In general, 500 ml of test solution were used for each test. A commercial saturated calomel electrode (SCE) was used as a reference electrode for all experiments. The auxiliary electrode was a bright platinum 1mm diameter wire, area 2 cm^2 (Figure 1).

2.3. Electrochemical Procedures Polarization tests were carried out with an ACM potentiostate (ACM Instruments Co) connected to a scanning system. The scanning rate of all potential sweep in Linear Polarization Resistance (LPR) tests, was 10 mV/min and the scanning range was from-10 to 10 mV around the corrosion potential. The sweeping rate of all potential sweeps in E-logi diagrams was 30 mV/min and the scanning range was from-250 to 250 mV around the corrosion potential. Each scanning began from the cathodic region and stopped at the end anodic potential. During short term measurement of inhibitor performance LPR measurements were measured every hour for 6 hours. During these measurements, electrochemical cells were under the control of the CO_2 environment.

TABLE 1. Chemical Composition of Carbon Steel (wt %).

C	Si	S	P	Mn	Ni	Cr	Fe
0.19	0.27	0.010	0.13	1.10	0.10	0.43	Balance

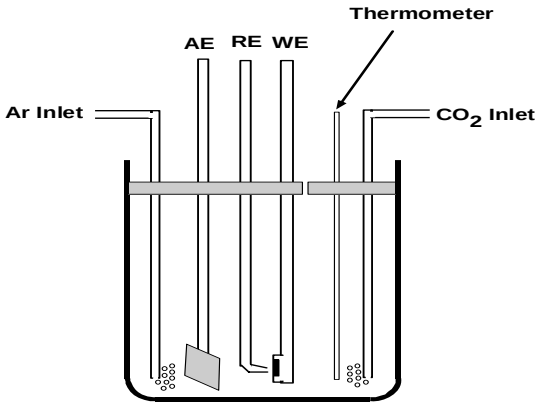

Figure 1. Corrosion test cell used in this work where, WE (working electrode), AE (Auxiliary electrode), RE (Reference electrode).

3. RESULTS AND DISCUSSION

The chemical composition of the tubing materials reveals that it is a low alloy steel containing very low detrimental elements (S and P). From corrosion point of view, such elements as Cr and Ni are considered beneficial. Morphological investigation of the specimen after etching in Nital shows that the alloy has undergone heat treatment followed by tempering. Detached, almost round, carbide particles dispersed in the ferittic matrix is evidence of such a heat treatment (Figures 2).

Linear Polarization Resistance (LPR), is a fast method for the evaluation of corrosion rates in a sample. This method is based on linear relationships between the potential and the current density which circulates across the metal/electrolyte interface, close to the corrosion potential. The polarization resistance (R_P) in $\Omega.cm^2$ is defined as follows:

$$R_P = \left(\frac{\partial E}{\partial i}\right)_{E_{corr}} = \frac{b_a.b_c}{2.3(b_a + b_c).i_{corr}} \quad (6)$$

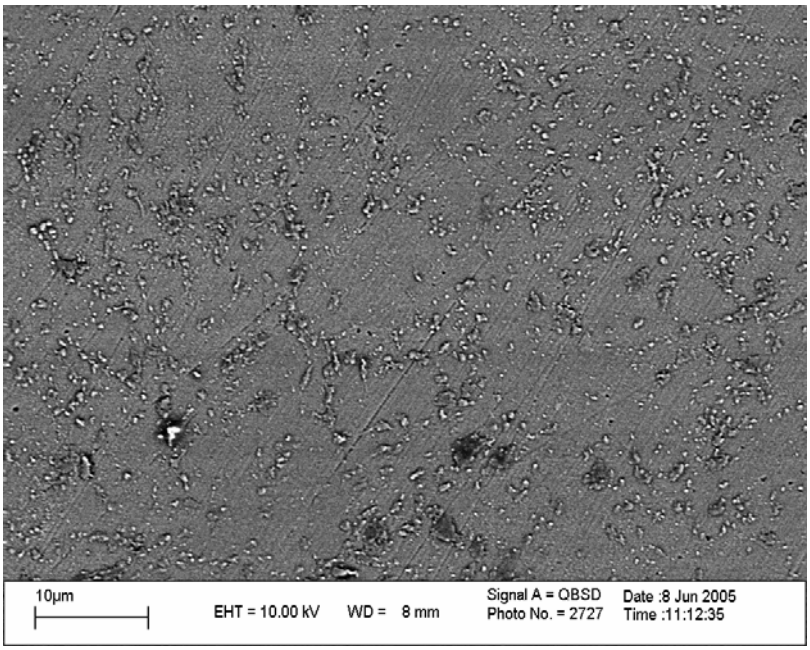

Figure 2. SEM micrograph of mild steel used in this work after etching in Nital.

where the corrosion current density in A/cm^2 is given by:

$$i_{corr} = \frac{b_a.b_c}{2.3(b_a + b_c)} \times \frac{1}{\left(\frac{\partial E}{\partial i}\right)_{E_{corr}}} = \frac{B}{R_P} \qquad (7)$$

Therefore Equation 7 gives a method of measuring the corrosion current density, provided the parameter R_P and B are known.

Potentiodynamic polarization of the working electrode beyond the corrosion potential and close to it is presented in E-log i and LPR curves in Figures 3 and 4. It is well known that corrosion of steel in CO_2 environments are affected by the formation of surface film mainly iron carbonate. Since decomposition of bicarbonate (HCO_3^-) ions is facilitated by an increase in temperature according to the following reaction:

$$2HCO_3^- \rightarrow CO_3^{-2} + H_2O + CO_2 \qquad (8)$$

Therefore iron carbonate ($FeCO_3$) easily precipitates as the result of increasing temperature from ambient to 60°C. Formation of such a film can suppress and acts as a barrier for further dissolution of iron [8]. This fact is evident in E-log i and LPR curves presented in Figure 3 and 4 where the polarization curves have shifted to the right (Figure 3) and the slope of E-i has been increased in Figure 4. A close look to both curves shows that increasing temperature from room temperatures to 60°C has affected the anodic current rather than the cathodic current density due to local formation of Fe^{2+} and precipitation of carbonate precipitate at the anodic sites. Measuring corrosion potential of a working electrode is a simple and meaningful investigation in corrosion inhibitors. According to mixed theory potential, a corrosion potential is a unique potential associated with the total anodic and cathodic reactions in the system. The typical variation of the working electrode corrosion potential against a reference electrode is illustrated in Figure 5. Considering the corrosion potential of the test solution and comparing it with the standard electrochemical potential for the most possible cathodic reactions in the system (electrochemical reactions of 2a, 2b, and 2c), it reveals that the supporting cathodic reactions for the anodic reaction are mainly

Equation 2a and 2c. Addition of a corrosion inhibitor into the system increases the corrosion potential towards more noble values. Any interaction of corrosion inhibitors with the anodic site causes an increase in the anodic Tafel slope or a decrease in the anodic exchange current density which is responsible for shifting the corrosion potential to more noble values. In fact the inhibitor acts as an anodic inhibitor. Change of corrosion potential towards more noble values at with the presence of corrosion inhibitors is evident from considering zero net current density of E-log i curves in Figure 6. The microstructure of tubing steel used in this work that consists of a ferritic matrix containing detached carbide particles dominates the inhibitor action in the corrosion process. This is worth noting that cathodic inhibitors act well in steel microstructures consisting of ferrite and pearlite phases due to adsorption on cementite leading to polarization of cathodic branches of the E-logi curve while anodic inhibitors are acting well in the ferritic or martensitic structures [20]. The addition of an inhibitor causes a shift of potentiodynamic polarization curves to left which means lowering corrosion current density. Comparing the polarization curves at the presence and absence of an inhibitor reveals that an inhibitor causes a decrease in exchange current densities rather than Tafel slopes. Similar trends in decreasing corrosion current density are evident in LPR measurements of working electrodes in test solutions with different concentrations of inhibitors (Figure 7).

In order to clarify that the inhibitor action on the surface is due to adsorption, the Lungmuir adsorption isotherm was calculated. The apparent corrosion rate on inhibited steel is proportional to the ratio of surface converge (θ) and that which is not covered (1-θ) by the inhibitor. Surface coverage values have been evaluated in different concentrations of inhibitor under the study of corrosion rates in uninhibited and inhibited solutions by means of the following equation:

$$\theta = 1 - \frac{i_{inhibited}}{i_{nuninhibited}} \qquad (9)$$

Where $i_{inhibited}$ and $i_{uninhibited}$ are the corrosion rates obtained from extrapolation of E-log i curves at the presence and the absence of inhibitor. θ is also

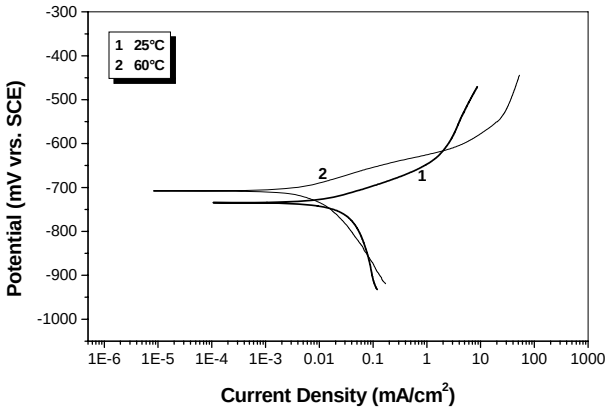

Figure 3. Potentiodynamic polarization curves of working electrode in CO_2 saturated test solution at 25°C (1) and 60°C (2).

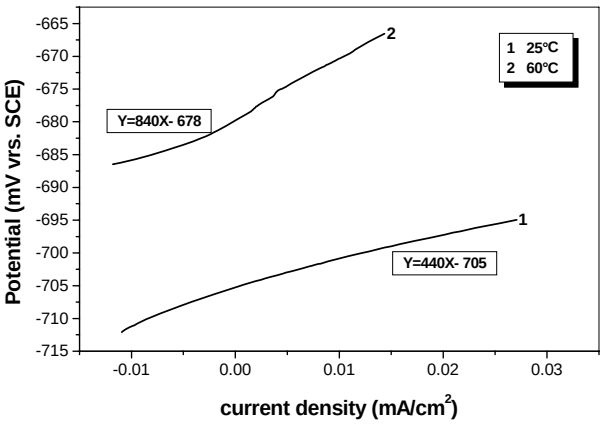

Figure 4. E-i curves of linear polarization resistance (LPR) of working electrode in CO_2 saturated solution at (1) 25°C and (2) 60°C.

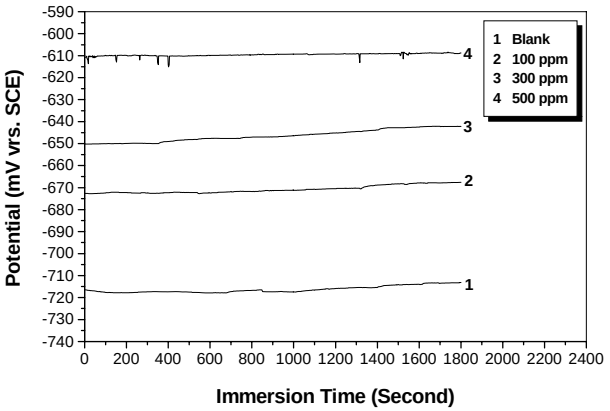

Figure 5. Variation of corrosion potential with immersion time for blank solution and blank solution containing different concentrations of inhibitor at room temperature.

calculated from the R_P measurements using the following equation:

$$\theta = 1 - \frac{R_{P_{uninhibited}}}{R_{P_{inhibited}}} \quad (10)$$

Where $R_{Puninhibited}$ and $R_{Pinhibited}$ are the polarization resistances of the working electrode at the absence and the presence of inhibitor, respectively. The Langmuir adsorption isotherm may be expressed as [20]:

$$\theta = \frac{Kc}{Kc + 1} \quad (11)$$

Where K is the equilibrium constant for the adsorption process, c is the concentration of inhibitor and θ is surface coverage:

$$\frac{c}{\theta} = \frac{1}{K} + c \quad (12)$$

Figure 8 illustrates the plot of c/θ versus inhibitor concentration (c) using different measurement methods. The straight line with a slope very close to unity, indicates that adsorption of the investigated commercial inhibitor on steel/saturated CO_2 solution obeys the Lungmuir adsorption isotherm. The effect of temperature on the corrosion inhibitor adsorption was also investigated by potentiodymic polarization and LPR measurement. The polarization curves and LPR of the specimen at presence of a 300 ppm inhibitor at room temperature and 60˚C are shown in Figure 9 and 10 respectively. The corrosion rate of sample decreases and R_P increases with the increasing of the temperature. It is evident that the increasing of the temperature improves surface chemisorptions of this inhibitor.

In order to find out the variation of inhibitive properties of the inhibitor with time, the variations of LPR with time were measured for a constant 300 ppm concentration of inhibitor in a saturated CO_2 environment. Figures 11 and 12 represent these variations. Two distinguished points can be addressed here. Gradual increase of the slope of the curve reveals the adsorption of the inhibitor. This increase in the slope is greater for the first four hours and then declines. In fact there is no

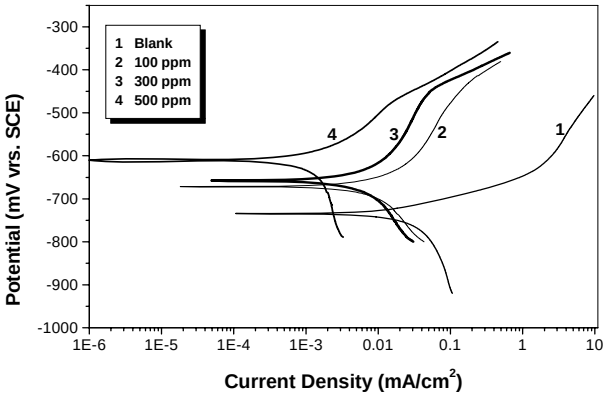

Figure 6. Potentiodynamic polarization curves of working electrode in the absence and the presence of inhibitor with different concentrations.

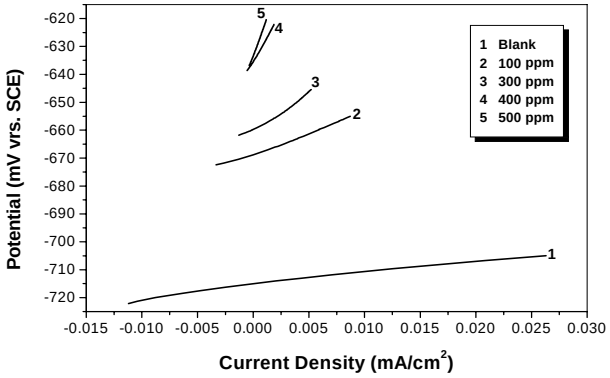

Figure 7. E-i curves of linear polarization resistance (LPR) of working electrode in solutions with different concentrations of inhibitor.

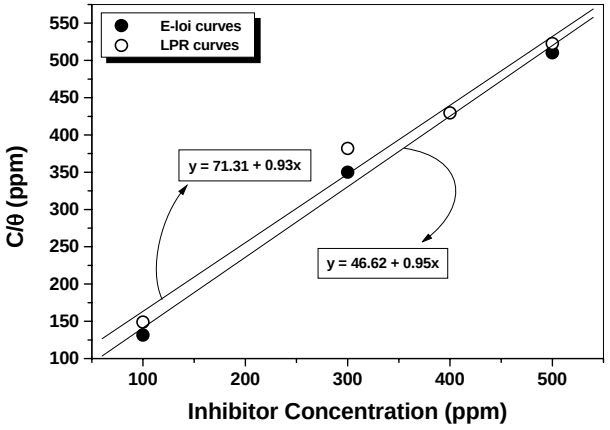

Figure 8. Curve fitting of corrosion data of working electrode in the presence of inhibitor to Lungmuir isotherm.

meaningful difference between the slopes of the E-i curve for 5 hrs-6 hrs of immersion. On the other hand, by comparing the corrosion potentials associated with the zero current density for different immersion times show, for a particular concentration of inhibitor (here 300 ppm), the mechanism of inhibitor action on the surface is dissimilar with its mechanism for different inhibitor concentrations. Figure 11 shows a gradual small decreasing in the corrosion potential associated with the zero current density from -683 to-691 mV after 6 hrs of immersion of the specimen in the solution containing 300ppm inhibitor. This may prove the possible domination of cathodic polarization of the system rather than anodic polarization. Considering the variation of the E-i slope with time and according to the following equation, the inhibitor efficiency (η) can be calculated.

$$\%\eta = 1 - \left(\frac{(R_p)_{\text{uninhibited}}}{(R_p)_{\text{inhibited}}} \right) \quad (13)$$

Where $(R_P)_{\text{inhibited}}$ and $(R_P)_{\text{uninhibited}}$ are the polarization resistance at the presence and absence of inhibitor. Figure 13 illustrates the variation of inhibitor efficiency with immersion time at the presence of the 300 ppm inhibitor. This result shows that the inhibitor efficiency depends on the exposure time. The longer the exposure time, the more adsorption of inhibitor occurs on the surface and then surface coverage by the compact film of inhibitor improves. A more compact film obtained from a longer immersion time gives a better corrosion inhibition.

4. CONCLUSIONS

The main conclusions drawn from this study are:

- Potentiodynamic and LPR measurements of gas well tubing steel in saturated CO_2 environment showed that increasing temperature from the room to 60°C causes a decrease in the steel corrosion rate.
- The inhibition effect of Imidazoline

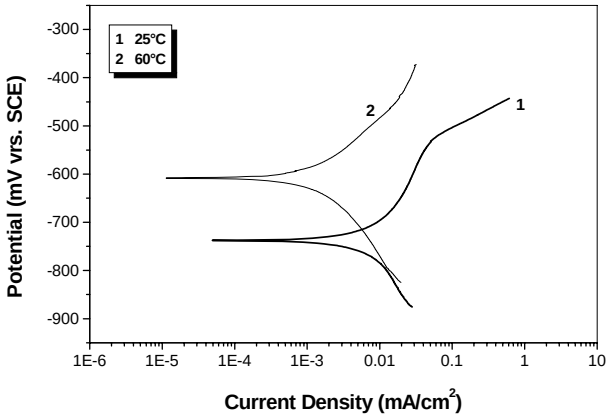

Figure 9. Potentiodynamic polarization curves of working electrode in solution with 300 ppm concentration of inhibitor at (1) 25°C and (2) 60°C.

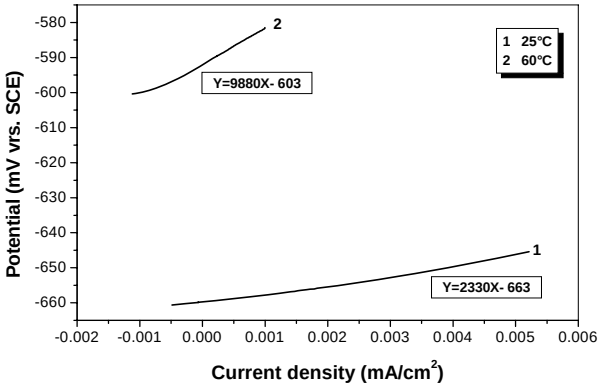

Figure 10. E-i curves of linear polarization resistance (LPR) of working electrode in solution containing 300 ppm inhibitor at (1) 25°C and (2) 60°C.

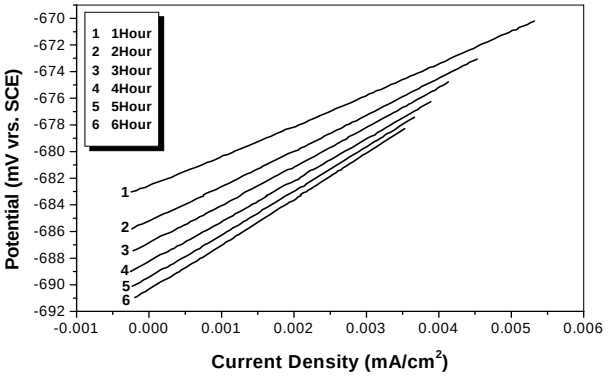

Figure 11. E-i curves of linear polarization resistance (LPR) of working electrode in solution containing 300 ppm inhibitor for various immersion time.

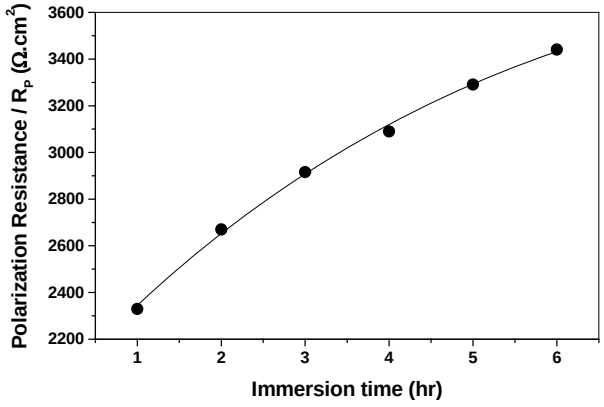

Figure 12. Variation of R_P value with immersion time in solution containing 300 ppm inhibitor at room temperature.

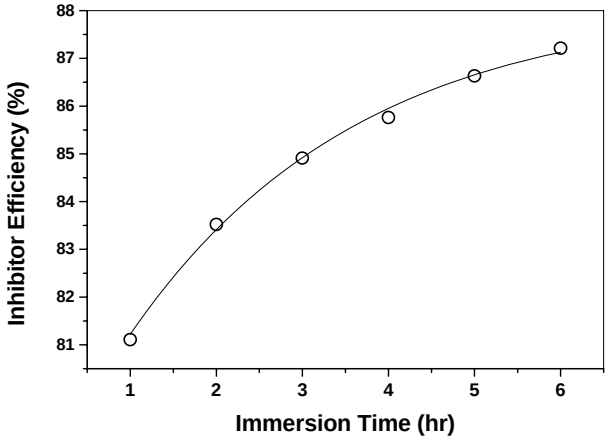

Figure 13. Variation of inhibitor efficiency with immersion time in solution containing 300 ppm inhibitor at room temperature.

based commercial inhibitor increases with the increase in inhibitor concentration in the media.

- The inhibition is due to adsorption of inhibitor molecules on the steel surface on the active sites due to fitting measurement data to Lungmuir adsorption isotherm.
- Short term measurement of LPR with 300ppm inhibitor concentration indicated that the adsorption mechanism is time dependent for constant inhibitor concentration.

5. REFERENCES

1. Wua, S. L., Cuia, Z. D., Heb, F., Baic, Z. Q., Zhua, S. L. and Yang, X. J., "Characterization of the surface film formed from carbon dioxide corrosion on N80 Steel", ***Materials Letters***, Vol. 58, (2004), 1076-1081.
2. Nestle, A., "Corrosion inhibitors in petroleum production primary recovery", ***NACE Publication***, (1973), 61-75.
3. Heue, J. K. and Stubbins, J. F., "An XPS characterization of $FeCO_3$ films from CO_2 corrosion", ***Corrosion Science***, Vol. 41, (1999), 1231-1243.
4. Wua, S. L., Cuia, Z. D., Zhaob, G. X., Yanb, M. L., Zhua, S. L. and Yang, X. J., "EIS study of the surface film on the surface of carbon steel from supercritical carbon dioxide corrosion", ***Applied Surface Science***, Vol. 228, (2004), 17–25.
5. Linter, B. R. and Burstein, G. T., "Reactions of pipeline steels in carbon dioxide solutions", ***Corrosion Science***, Vol. 41, (1999), 117-139.
6. Schmitt, G. and Rothman, B., "Inhibition of carbon-dioxide corrosion of equipment of the petroleum and gas industry", ***Materials and Corrosion***, Vol. 28, (1977), 816.
7. Gray, L. G. S., Anderson, B. G., Danysh, M. J. and Tremaine, P. R., "Effect of pH and temperature on the mechanism of carbon steel corrosion by aqueous carbon dioxide", Corrosion 190, paper 40, Houston TX: ***NACE International***, (1993), 1-26.
8. Dugstad, A., "The importance of $FeCO_3$ supersaturation of carbon steel", Corrosion 92, paper 14, Houston TX: ***NACE International***, (1992), 43-51.
9. Crolet, J. L. and Bonis, M., "The role of acetate in CO_2 corrosion", Corrosion 83, paper 160, Houston TX: ***NACE International***, (1983), 1-16.
10. Crolet, J. L., Thevenot, N. and Nesic, S., "Role of conductive corrosion products in the protectiveness of corrosion layers", ***Corrosion***, Vol. 54, (1998), 194-203.
11. Zhang, X., Wang, F., He, Y. and Du, Y., "Study of the inhibition mechanism of imidazoline amide on CO_2 corrosion of Armco iron", ***Corrosion Science***, Vol. 43, (2001), 1417-1431.
12. Heeg, B. and Klenerman, D., "Persistency of corrosion inhibitor films on c - steel under multiphase flow conditions, part II: optical SHG and electrochemical studies", ***Corrosion Science***, Vol. 4, (1998), 1313-1329.
13. Cruz, J., Mart_ınez, R., Genesca, J. and Garcia - Ochoa, E., "Experimental and theoretical study of 1 - (2-ethylamino) - 2 - methylimidazoline as an inhibitor of carbon steel corrosion in acid media", ***Journal of Electronalytical Chemistry***, Vol. 566, (2004), 111-121.
14. Chen, Y. and Jepson, W. P., "EIS measurement for corrosion monitoring under multiphase flow conditions", ***Electrochimica Acta***, Vol. 44, (1999), 4453-4464.
15. Hong, T., Sun, Y. H. and Jepson, W. P., "Study on corrosion inhibitor in large pipelines under multiphase flow using EIS", ***Corrosion Science***, Vol. 44, (2002), 101-112.
16. Lopez, D. A., Simison, S. N. and De Sanchez, S. R., "The influence of steel microstructure on CO_2

corrosion. EIS studies on the inhibition efficiency of benzimidazole", ***Electrochemical Acta***, Vol. 48, (2003), 845-854.
17. Zhang, X., Wang, F., He, Y. and Du, Y., "Study of the inhibition mechanism of imidazoline amide on CO_2 corrosion of Armco iron", ***Corrosion Science***, Vol. 43, (2001), 417-1431.
18. Item No. 24007, "Wheel test method used for evaluation film-persistent corrosion inhibitors for oiled field application", NACE International Publication 1D182, (2005).
19. Mora-Mendoza, J. L. and Turgoose, S., "Fe_3C influence on the corrosion rate of mild steel in aqueous CO_2 systems under turbulent flow conditions", ***Corrosion Science***, Vol. 44, (2002), 1223-1246.
20. Lopez, D. A., Simison, S. N. and de Sanchez, S. R., "Inhibitors performance in CO_2 corrosion EIS studies on the interaction between their molecular structure and steel microstructure", ***Corrosion Science***, Vol. 47, (2005), 735-755.
21. Harek, Y. and Larabi, L., "Corrosion Inhibition of Mild Steel in 1 mol dm^{-3} HCl by oxalic N - Phenyhydrazide N' - Phenylthiosemicarbazide", ***Kem. Ind.***, Vol. 53, No. 2, (2004), 55–61.